Letter

# Resonant binding of dielectric particles to a metal surface without plasmonics

Evgeny Bulgakov,[1,2] Konstantin Pichugin,[1] and Almas Sadreev[1]
[1]*Kirensky Institute of Physics Federal Research Center KSC SB RAS, 660036 Krasnoyarsk, Russia*
[2]*Reshetnev Siberian State University of Science and Technology, 660037 Krasnoyarsk, Russia*

(Received 8 March 2021; accepted 19 May 2021; published 26 May 2021)

A high index dielectric spherical particle supports the high-$Q$ resonant Mie modes that result in a regular series of sharp resonances in the radiation pressure. The presence of a perfectly conducting metal surface transforms the Mie modes into extremely high-$Q$ magnetic bonding or electric antibonding modes for the close approach of a sphere to a surface. We show that an electromagnetic plane wave with normal incidence results in repulsive or attractive resonant optical forces relative to a metal for the excitation of electric bonding or magnetic antibonding resonant modes, respectively. A magnitude of resonant optical forces reaches the order of 1 nN of magnitude for micron-sized silicon particles and a power of light 1 mW/$\mu$m$^2$ that exceeds the gravitational force by four orders. However, what is the most remarkable is there are steady positions for a sphere between the pulling and pushing forces that give rise to the resonant binding of the sphere to a metal surface.

DOI: 10.1103/PhysRevA.103.L051501

## I. INTRODUCTION

The illumination of a dielectric spherical particle by a plane wave with a definite wave vector gives rise to radiation pressure which drags the particle along the wave vector because of the preservation of momentum. Irvine has shown that a regular series of sharp resonances in the radiation pressure superimposes on this placid background of radiation pressure caused by the excitation of Mie resonant modes with a high-$Q$ factor in dielectric spherical particles [1]. In 1977, Ashkin and Dziedzic reported the first precise observation of these resonances based on force spectroscopy [2]. The illumination of spherical particles by spatially structured beams can even pull particles because of the absence of definite longitudinal momentum [3–5]. However, irrespectively there are no equilibrium positions for particles over the axis of a beam.

Obviously, the presence of a surface which reflects an incident plane wave can drastically change a situation with the equilibrium positions for the particles, i.e., the surface can trap outside particles. A dielectric surface can trap particles using the evanescent tails of waveguide modes [6] while a metal surface can trap particles due to the unidirectional excitation of surface plasmonic waves (SPWs) by oblique plane waves [7–14]. A similar way to trap dielectric particles is based on the excitation of SPWs and volumetric hyperbolic waves on hyperbolic surfaces [15]. A key issue in particle trapping by evanescent tails is the formation of a stable equilibrium in the transverse direction which is rather close to the surface while in the direction along the surface the stability of the particles remains in question.

In the present Letter we show that a metal surface can trap dielectric spheres with a high refractive index (silicon) in two ways. In the first way the surface strongly absorbs the spheres at a minimal distance around magnetic antibonding resonances. The particles can also be trapped at finite distances between the surface and spheres when a plane wave excites the high-$Q$ electric bonding modes, causing levitation of the spheres over a metal surface. Resonant trapping occurs for a perfectly reflecting metal as for a real metal (silver) where electromagnetic waves scattered by a sphere excite the surface plasmon waves, which however are not relevant for resonant trapping at normal incidence of the plane waves. For the case of a perfectly conducting metal the problem of scattering can be solved by resorting to image theory, according to which a field scattered into an accessible half space by a sphere in the presence of a reflecting surface coincides with a field scattered by a compound object that includes the particle and its image, provided the exciting field is the superposition of the actual incident field and of the field that comes from the image source [16]. Therefore the problem can be considered as a scattering of electromagnetic (EM) waves by two spheres. The presence of a second particle or any scattering object leads to multiple scattering between the object and particle and can then lead to the optical binding of the particle to the object even under the illumination of one beam. This peculiar manifestation of optical forces is often referred to as optical binding, and it was first discovered by Burns *et al.* on a system of two plastic spheres in water in 1989 [17]. For the case of a silver metal substrate we use a multipolar approach by Takemori *et al.* [18] which was subsequently compared to results obtained by COMSOL PHYSICS.

Sharp features in the force spectroscopy, causing a mutual attraction or repulsion between successive photonic crystalline layers of dielectric spheres under illumination of a plane wave, have been presented by Antonoyiannakis and Pendry [19]. Each layer is specified by extremely narrow resonances which transform into bonding and antiboding resonances for the closely approaching layers. It was revealed that lower-frequency bonding resonance forces push the two layers together and higher-frequency antibonding

 

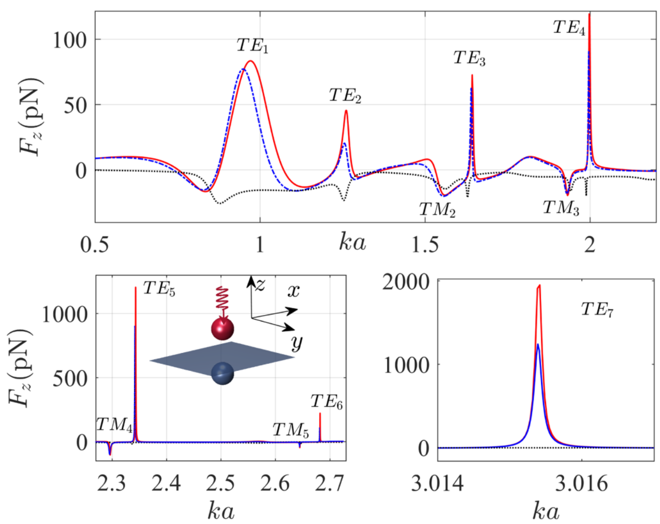


FIG. 1. Force normal to a silver surface acting on a silicon sphere with radius $a = 0.55$ $\mu$m and refractive index $n = 3.464$ at a distance $L = 1.2a$ between the center of the sphere and surface under illumination of a plane wave with intensity $P = 1$ mW/$\mu$m$^2$. The black dotted line shows the radiation pressure acting on a bare sphere, the red solid line shows the case of an ideal metal, and the blue dashed-dotted line shows the case of a silver metal with refractive index $n = 0.14 + 11i$ at $\lambda = 1.5$ $\mu$m. Subindices enumerate the orbital momentum $l$ of the Mie resonances of a bare sphere. The inset shows a sphere above the metal surface and its image below.

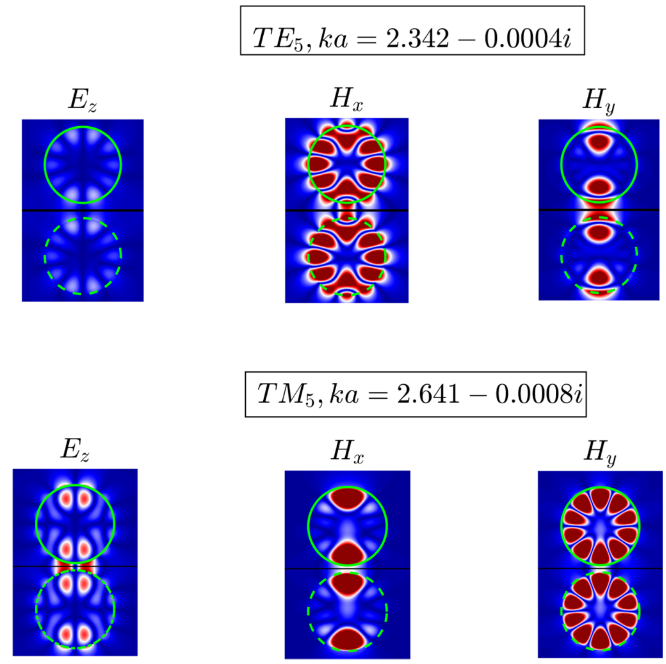


FIG. 2. Absolute values of components of the EM field of resonant modes at a distance $L = 1.2a$ from an ideally conducting surface shown by the black solid lines with corresponding complex resonant frequencies.

resonance forces pull them apart. These conclusions are based on an analogy of the Maxwell's equations with the quantum mechanics, in particular with molecular orbitals. Later we reported these disclosures for coupled photonic crystal slabs [20], two planar dielectric photonic metamaterials [21], two silicon spheres [22,23], and two coaxial disks [24]. Similarly for the case of a dielectric sphere with a large refractive index at a perfectly conducting surface the high-$Q$ Mie resonant modes transform into bonding transverse magnetic (TM)-type or antibonding transverse electric (TE)-type modes which give rise to attractive or repulsive resonant forces because of the boundary conditions. What is important is that these forces considerably exceed by two orders of magnitude the resonant pushing forces in the case of a bare sphere [1,2].

## II. OPTICAL FORCES

The problem is solved by the $T$-matrix approach [25] that allows us to calculate the optical force acting on the particle via the stress tensor [26],

$$F_\alpha = \int T_{\alpha\beta} dS_\beta,$$

$$T_{\alpha\beta} = \frac{1}{4\pi} E_\alpha E_\beta^* - \frac{1}{8\pi}\delta_{\alpha\beta}|\mathbf{E}|^2 + \frac{1}{4\pi} H_\alpha H_\beta^* - \frac{1}{8\pi}\delta_{\alpha\beta}|\mathbf{H}|^2. \quad (1)$$

In what follows we consider a plane wave incident normally to the metal surface as shown by the red wavy line in the inset of Fig. 1. That makes the system equivalent to two identical spheres in air in the superposed standing wave $E_0 \vec{e}_x \sin kz$ with an even solution for $E_z$ and an odd solution for $H_z$. Respectively we have odd or even solutions for the tangential components of EM fields. The results of the calculations are presented in Fig. 1 where the dotted line shows the radiation-pressure force onto a bare sphere in air with peaks located at the Mie resonant modes indexed by the orbital momentum $l$. That approach differs from the consideration of optical forces effecting the dielectric particles by metal surfaces due to the excitation of the surface plasmon modes by oblique plane waves [8–10,27].

When two spheres in air are approaching, the Mie resonances of each sphere are split and their resonant modes are hybridized, forming bonding and antibonding resonant modes irrespective of polarization. Respectively, a sign of optical force between two spheres follows these modes [23]. For the present case of one sphere near the metal surface the Mie resonances are not split when the sphere approaches the surface but are only shifted, as force spectroscopy shows in Fig. 1. The reason is related to the odd standing-wave field $\sin kz$ affecting the sphere and its image can excite only odd resonant modes for tangential components of the electric field. One can see that for the TE resonances the shift is positive with repulsive optical forces while for the TM resonances the shift is negative with attractive forces. In order to comprehend this rule we show in Fig. 2 the resonant modes $TE_5$ and $TM_5$ from a perfectly conducting surface. For the $TE_5$ one can see the transverse components of the magnetic field dominate compared to the $E_z$ in space between the sphere and surface. Therefore the stress-tensor component can be approximated as $T_{zz} \approx -\frac{1}{8\pi}(|H_x|^2 + |H_y|^2) < 0$. Then we can consider that the force $F_z \sim T_{zz}\sigma > 0$. Here, $\sigma$ is a small area at the bottom of the sphere directed oppositely to the $z$ axis and inside of which the magnetic field dominates. Therefore the excitation

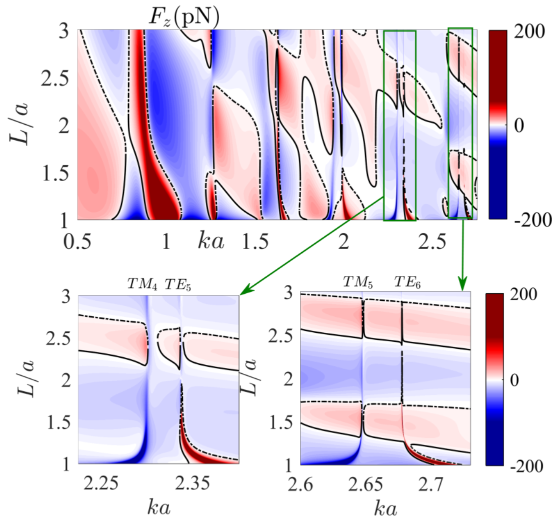


FIG. 3. The optical force between a sphere and an ideally conducting surface vs the frequency and distance for illumination of the plane mode with normal incidence. Dashed (solid) lines show steady (unsteady) positions of the sphere.

of the TE resonances results in a positive force, i.e., the repulsive force that indeed fully agrees with Fig. 1 for TE resonances. As for the resonant mode $\mathrm{TM}_5$ one can see from Fig. 2 that $E_z$ dominates over the magnetic field at the bottom of the sphere to have $T_{zz} \approx \frac{1}{8\pi}(|E_z|^2 - |H_x|^2 - |H_y|^2) > 0$. Therefore the excitation of the TM resonances result in an attractive force, as also agrees with Fig. 1. These results hold also for the case of a real silver metal surface with a refractive index $n = 0.14 + 11i$ with however slightly reduced values of the optical force, as shown in Fig. 1 by the blue dashed-dotted line.

In Fig. 3 we show the results of calculations of the optical force versus the frequency of a plane wave with normal incidence and power 1 mW/$\mu$m$^2$ and distance between the sphere and metal surface. Because of the oscillating behavior of the optical force [23,28] one can see that attractive resonant forces around the $\mathrm{TM}_{l-1}$ resonances are substituted by repulsive forces around the $\mathrm{TE}_l$ resonances. Similar to Figs. 1 and 3 manifests force spectroscopy by Ashkin and Dziedzic [2]. Figure 3 shows also equilibrium positions versus the frequency and the distance between the sphere and metal surface.

The insets in Fig. 3 demonstrate a considerable enhancement of optical forces up to hundreds of pN that exceed the gravitational forces by four orders for micron-sized silicon particles. Expectedly, such an enormous enhancement of resonant forces is the result of extremely large $Q$ factors of the resonances as was considered in Refs. [19,29]. If the resonant amplitudes of EM fields are proportional to $\sqrt{Q}$, the resonant forces grow linearly with $Q$, as follows from Eq. (1). On the other hand, the $Q$ factor of the Mie modes rapidly grows with large $l$ [30] to expect similar behavior for the radiation pressure. However, as shown by the dotted line in Fig. 1, we have no such dependence of peaks of the radiation pressure on $l$. Besides the $Q$ factor, the coupling constant of the incident plane field with the corresponding resonant mode contributes to the resonant optical force. Because of the increase of the number of nodal surfaces in the resonant modes with $l$, the

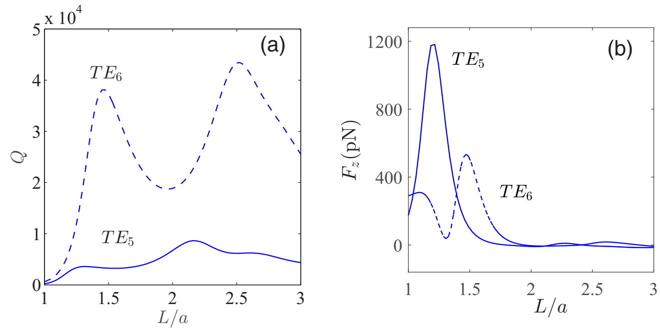


FIG. 4. (a) The $Q$ factor and (b) resonant force, vs the distance between a particle and metal silver surface for the case of excitation of the $\mathrm{TE}_5$ and $\mathrm{TE}_6$ resonant modes by a plane wave with power 1 mW/$\mu$m$^2$.

coupling has a tendency to decrease. In particular, Liu *et al.* have observed already that the higher-$Q$ state exhibits a much weaker coupling to the external radiation [29]. Figure 4 also demonstrates the absence of a strict correlation between the $Q$ factor and force in the present case. Moreover, the presence of a metal surface contributes to a difference between forces at the top of a sphere and at the bottom that complicates the behavior of the resonant forces with $l$. For example, forces resulting by excitation of the $\mathrm{TM}_5$ and $\mathrm{TE}_6$ resonances yield forces by the $\mathrm{TM}_4$ and $\mathrm{TE}_5$ resonances.

### III. RESONANT SORTING OF SPHERES

The subplots of force around resonances with high index $l$ in Fig. 3 demonstrate that the equilibrium positions of a sphere relative to a metal surface can be resonant over $L$, which however are crossed by the areas almost independent of $L$. In order to see these observations in a more comprehensive way, we present the potential relief versus frequency and distance between a sphere and metal surface by integrating the force $F_z$ over $z$. The fragment of potential is shown in Fig. 5(a), which demonstrates an extremely deep confining potential around the electric bonding resonance $\mathrm{TE}_5$ and a large potential barrier absorbing the sphere at the metal surface if the frequency of incident light is close to the magnetic antibonding resonance $\mathrm{TM}_4$. The potentials around other resonances show similar behaviors. One can see that both cases enormously

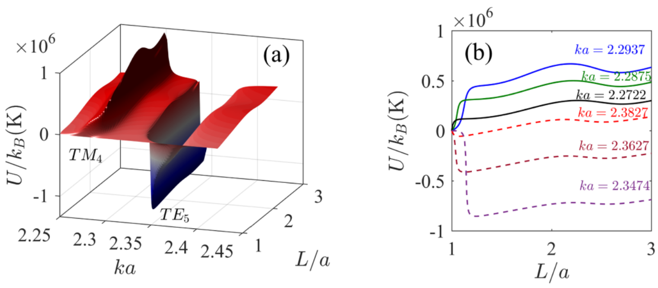


FIG. 5. (a) Potential relief in degrees Kelvin normalized to the Boltzmann constant $k_B$ vs the frequency of incident light and distance between a perfectly conducting metal surface and center of a sphere in the vicinity of $\mathrm{TM}_4$ and $\mathrm{TE}_5$ resonances.

exceed room temperature. Therefore we can conclude that a metal surface can strongly absorb silicon spherical particles under normal incidence of a plane wave with a relatively small power of 1 mW/$\mu$m$^2$ provided that a laser beam excites the magnetic antibonding resonances $\mathrm{TM}_l$. That case is shown by the solid lines in Fig. 5(b). On the other hand, excitation of the electric bonding resonances gives rise to the levitation of spheres over the metal surface at definite distances as dependent on the orbital momentum $l$. That case is shown by the dashed lines in Fig. 5(b). Since the frequency is measured in terms of the sphere radius as $ka$, we can conclude that the processes of binding or repulsion of spheres are very sensitive to the sizes of the particles as Fig. 3 clearly shows. If we were to assume that the spheres of different sizes are flowing in a viscous liquid, a plane wave with a definite frequency will mostly repel particles except those particles whose radii fit to the $\mathrm{TM}_l$ resonances. Therefore some fracture of spheres of definite radii will be trapped on definite distances from the metal surface, which can pave a way for the resonant sorting of particles by size. That brings a different potential to exploit these results for optical trapping and for optical resonant sorting [31–35].

One can expect that the larger optical forces will take away the sphere into positions far from resonance in order to diminish the forces. Indeed, this conclusion holds for resonances with lower $l$. However, for extremely high-$Q$ resonances with angular momentum $l = 5, 6, \dots$ one can see that the steady distances of silicon spheres from the metal surface are close to the resonant frequencies. That tendency for particles to be placed into positions close to resonance was revealed also in a Fabry-Pérot resonator with movable mirrors [36].

## ACKNOWLEDGMENTS

The work was supported by Russian Foundation for Basic Research Project No. 19-02-00055.


[1] W. Irvine, Light scattering by spherical particles: Radiation pressure, asymmetry factor, and extinction cross section, J. Opt. Soc. Am. **55**, 16 (1965).

[2] A. Ashkin and J. M. Dziedzic, Observation of Resonances in the Radiation Pressure on Dielectric Spheres, Phys. Rev. Lett. **38**, 1351 (1977).

[3] A. Novitsky and D. Novitsky, Negative propagation of vector Bessel beams, J. Opt. Soc. Am. A **24**, 2844 (2007).

[4] J. Chen, J. Ng, Z. Lin, and C. T. Chan, Optical pulling force, Nat. Photonics **5**, 531 (2011).

[5] H. Li, Y. Cao, L.-M. Zhou, X. Xu, T. Zhu, Y. Shi, C.-W. Qiu, and W. Ding, Optical pulling forces and their applications, Adv. Opt. Photonics **12**, 288 (2020).

[6] H. Jaising and O. Hellesø, Radiation forces on a Mie particle in the evanescent field of an optical waveguide, Opt. Commun. **246**, 373 (2005).

[7] G. Volpe, R. Quidant, G. Badenes, and D. Petrov, Surface Plasmon Radiation Forces, Phys. Rev. Lett. **96**, 238101 (2006).

[8] M. Righini, A. Zelenina, C. Girard, and R. Quidant, Parallel and selective trapping in a patterned plasmonic landscape, Nat. Phys. **3**, 477 (2007).

[9] X. Yang, Y. Liu, R. F. Oulton, X. Yin, and X. Zhang, Optical forces in hybrid plasmonic waveguides, Nano Lett. **11**, 321 (2011).

[10] M. Petrov, S. Sukhov, A. Bogdanov, A. Shalin, and A. Dogariu, Surface plasmon polariton assisted optical pulling force, Laser Photonics Rev. **10**, 116 (2015).

[11] A. Ivinskaya, M. Petrov, A. Bogdanov, I. Shishkin, P. Ginzburg, and A. Shalin, Plasmon-assisted optical trapping and anti-trapping, Light: Sci. Appl. **6**, e16258 (2016).

[12] S. Sukhov and A. Dogariu, Non-conservative optical forces, Rep. Progr. Phys. **80**, 112001 (2017).

[13] A. V. Maslov, Levitation and propulsion of a Mie-resonance particle by a surface plasmon, Opt. Lett. **42**, 3327 (2017).

[14] A. Maslov, Binding of resonant dielectric particles to metal surfaces using plasmons, Ann. Phys. **532**, 2000129 (2020).

[15] A. Ivinskaya, N. Kostina, A. Proskurin, M. Petrov, A. Bogdanov, S. Sukhov, A. Krasavin, A. Karabchevsky, A. Shalin, and P. Ginzburg, Optomechanical manipulation with hyperbolic metasurfaces, ACS Photonics **5**, 4371 (2018).

[16] F. Borghese, P. Denti, and R. Saija, in *Scattering from Model Nonspherical Particles*, edited by K. Yasumoto (Springer, Berlin, 2007).

[17] M. M. Burns, J.-M. Fournier, and J. A. Golovchenko, Optical Binding, Phys. Rev. Lett. **63**, 1233 (1989).

[18] T. Takemori, M. Inoue, and K. Ohtaka, Optical response of a sphere coupled to a metal substrate, J. Phys. Soc. Jpn. **56**, 1587 (1987).

[19] M. I. Antonoyiannakis and J. B. Pendry, Mie resonances and bonding in photonic crystals, Europhys. Lett. **40**, 613 (1997).

[20] V. Liu, M. Povinelli, and S. Fan, Resonance-enhanced optical forces between coupled photonic crystal slabs, Opt. Express **17**, 21897 (2009).

[21] J. Zhang, K. F. MacDonald, and N. I. Zheludev, Giant optical forces in planar dielectric photonic metamaterials, Opt. Lett. **39**, 4883 (2014).

[22] T. Yano, Y. Tsuchimoto, R. P. Zaccaria, A. Toma, A. Portela, and M. Hara, Enhanced optical magnetism for reversed optical binding forces between silicon nanoparticles in the visible region, Opt. Express **25**, 431 (2017).

[23] E. N. Bulgakov, K. N. Pichugin, and A. F. Sadreev, Giant resonant enhancement of optical binding of dielectric particles, Phys. Rev. A **102**, 043518 (2020).

[24] E. N. Bulgakov, K. N. Pichugin, and A. F. Sadreev, Giant resonant enhancement of optical binding of dielectric disks, J. Opt. Soc. Am. B **37**, 3335 (2020).

[25] M. I. Mischenko, L. D. Travis, and A. A. Lacis, Scattering, Absorption and Emission of Light by Small Particles N.Y. 2004.

[26] M. I. Antonoyiannakis and J. B. Pendry, Electromagnetic forces in photonic crystals, Phys. Rev. B **60**, 2363 (1999).

[27] A. V. Maslov, Optical equilibrium for resonant particles induced by surface plasmons of two-dimensional materials, Phys. Rev. B **98**, 235414 (2018).
[28] V. Karásek, K. Dholakia, and P. Zemánek, Analysis of optical binding in one dimension, Appl. Phys. B **84**, 149 (2006).
[29] H. Liu, M. Panmai, Y. Peng, and S. Lan, Optical pulling and pushing forces exerted on silicon nanospheres with strong coherent interaction between electric and magnetic resonances, Opt. Express **25**, 12357 (2017).
[30] C. C. Lam, P. T. Leung, and K. Young, Explicit asymptotic formulas for the positions, widths, and strengths of resonances in Mie scattering, J. Opt. Soc. Am. B **9**, 1585 (1992).
[31] R. Applegate, J. Squier, T. Vestad, J. Oakey, and D. Marr, Optical trapping, manipulation, and sorting of cells and colloids in microfluidic systems with diode laser bars, Opt. Express **12**, 4390 (2004).
[32] K. Grujic, O. G. Hellesø, J. P. Hole, and J. S. Wilkinson, Sorting of polystyrene microspheres using a Y-branched optical waveguide, Opt. Express **13**, 1 (2005).
[33] O. Brzobohatý, V. Karásek, M. Šiler, L. Chvátal, T. Čižmár, and P. Zemánek, Experimental demonstration of optical transport, sorting and self-arrangement using a ‘tractor beam’, Nat. Photonics **7**, 123 (2013).
[34] Z. Li, S. Zhang, L. Tong, P. Wang, B. Dong, and H. Xu, Ultrasensitive size-selection of plasmonic nanoparticles by Fano interference optical force, ACS Nano **8**, 701 (2013).
[35] D. A. Shilkin, E. Lyubin, M. Shcherbakov, M. Lapine, and A. Fedyanin, Directional optical sorting of silicon nanoparticles, ACS Photonics **4**, 2312 (2017).
[36] A. F. Sadreev and E. Y. Sherman, Temporal oscillations of light transmission through dielectric microparticles subjected to optically induced motion, Phys. Rev. A **94**, 033820 (2016).